

Controlled absorption and all-optical diode action due to collisions of self-induced transparency solitons

Denis V. Novitsky*

*B. I. Stepanov Institute of Physics, National Academy of Sciences of Belarus,
Nezavisimosti Avenue 68, BY-220072 Minsk, Belarus*

(Dated: March 2, 2013)

We study inelastic collisions of counter-propagating self-induced transparency solitons in a homogeneously broadened two-level medium. The energy of the pulse can be almost totally absorbed in the medium due to asymmetric collision with a properly chosen control pulse. The medium state thus prepared demonstrates the property of an all-optical diode which transmits pulses from one direction and blocks from another. The saturation process of a controlled absorption effect, local-field correction influence, and the parameter ranges for the diode action are studied as well.

PACS numbers: 42.50.Md, 42.65.Sf, 42.65.Tg

I. INTRODUCTION

The problem of creation of all-optical diodes has been actively studied during recent years. Such systems, which transmit electromagnetic radiation only in one direction and block it in another, are usually based on asymmetrically constructed waveguides [1] or nonlinear photonic structures (see, for example, [2–5]). The use of left-handed materials [6] and asymmetrically absorbing systems [7] have been studied, among other possibilities. In other words, the all-optical diode action is commonly a consequence of the proper ordering of optical elements on microscopic scale (of the order of a light wavelength).

In this paper we propose a fundamentally different scheme of all-optical diode action. It is entirely based on nonlinear dynamics of the self-induced transparency (SIT) solitons in a homogeneously broadened, dense two-level medium. SIT is a well-known effect [8, 9], resulting in formation of stationary pulses (solitons) which propagate without change in their form. Our approach deals with collisions of counter-propagating SIT solitons. The effects of such collisions were partially studied in our previous work [10]. It was shown that under certain conditions, one of the colliding solitons can be almost entirely absorbed by the medium. We call this phenomenon *the controlled absorption* of the SIT soliton.

A large density of the two-level medium allows one to obtain the resulting effects on shorter distances. It is also useful for reducing the scope of the numerical calculations. The local-field effects need to be taken into account in this case. In Ref. [13] it was shown that they do not significantly affect the dynamics of a pulse with duration of femtosecond order. However, the local-field correction is taken into account here for generality; moreover, it is possible that it can somehow influence the dynamics on relatively long distances, as in our consideration. Therefore, we discuss this problem further as well.

The paper consists of the following sections. In Sec. II we consider the effect of controlled absorption of the SIT soliton in some detail. Section III is devoted to an explanation of our mechanism of all-optical diode action. In the Sec. IV we discuss the influence of pulse launch time, relaxation time, and medium density (as well as local field) on the demonstration of our effects. Finally, in Sec. V we make some concluding remarks.

II. CONTROLLED ABSORPTION

Propagation of light pulse in the dense two-level medium is governed by the system of semiclassical Maxwell-Bloch equations for population difference W , microscopic polarization R , and dimensionless Rabi frequency $\Omega' = \Omega/\omega = (\mu/\hbar\omega)E$ (i.e., the normalized electric field amplitude) [11, 12]:

$$\frac{dR}{d\tau} = i\Omega'W + iR(\delta + \epsilon W) - \gamma_2 R, \quad (1)$$

$$\frac{dW}{d\tau} = 2i(\Omega'^* R - R^* \Omega') - \gamma_1(W - 1), \quad (2)$$

$$\begin{aligned} \frac{\partial^2 \Omega'}{\partial \xi^2} - \frac{\partial^2 \Omega'}{\partial \tau^2} + 2i\frac{\partial \Omega'}{\partial \xi} + 2i\frac{\partial \Omega'}{\partial \tau} \\ = 3\epsilon \left(\frac{\partial^2 R}{\partial \tau^2} - 2i\frac{\partial R}{\partial \tau} - R \right), \end{aligned} \quad (3)$$

where $\tau = \omega t$ and $\xi = kz$ are dimensionless time and distance, respectively; $\delta = \Delta\omega/\omega$ the normalized detuning of the field carrier (central) frequency ω from the atomic resonance; $\gamma_1 = (\omega T_1)^{-1}$ and $\gamma_2 = (\omega T_2)^{-1}$ the rates of longitudinal and transverse relaxation, respectively; $k = \omega/c$ the wavenumber; c the light speed in vacuum; and $\epsilon = \omega_L/\omega = 4\pi\mu^2 C/3\hbar\omega$ is the normalized Lorentz frequency, where C is the concentration of the two-level atoms, and μ the component of transition dipole moment parallel to the polarization vector of the electric field. Here we assume without loss of generality that the background dielectric permittivity of the medium is unity (two-level atoms in vacuum). Note that in Eq. (3) we do not use the slowly varying envelope approximation

* dnovitsky@tut.by

(SVEA), while in Eq. (1) the term ϵW is responsible for the so-called local field correction (near dipole-dipole interaction) in a dense medium. The numerical approach used in this paper to solve Eqs. (1)–(3) can be found in Ref. [14].

We consider propagation of ultrashort pulses with Gaussian shape $\Omega = \Omega_p \exp(-t^2/2t_p^2)$, where t_p is the pulse duration. The amplitude of the pulses is measured in the units of the characteristic Rabi frequency $\Omega_0 = \sqrt{2\pi}/2t_p$, which corresponds to the so-called 2π pulse. In our calculations the values $T_1 = 1$ ns and $T_2 = 0.1$ ns are taken so that femtosecond pulses are in the regime of coherent interaction with the resonant medium. We use the following parameters of calculations which hold true throughout the paper: $\omega_L = 10^{11}$ s $^{-1}$, $\delta = 0$ (exact resonance), $\lambda = 2\pi c/\omega = 0.5$ μ m; the thickness of the medium $L = 1000\lambda$. All the pulses have the same duration $t_p = 50$ fs, which means that the only parameter governing pulse dynamics is its amplitude. One can estimate that a 2π pulse with such duration should have peak intensity of about 10 MW/cm 2 in the case of atomic dipole moments $\mu \sim 1$ D. The required concentration in this case is $C \sim 10^{19}$ cm $^{-3}$. However, the density and the peak intensity can be significantly reduced if the media with higher dipole moments is used (for example, a collection of quantum dots).

We start with the scheme of two ultrashort (coherent) counter-propagating pulses: the forward-propagating (FP) pulse with the initial amplitude Ω_{p1} and the backward-propagating (BP) one with Ω_{p2} (see Fig. 1). If their amplitudes are large enough, both pulses form self-induced transparency (SIT) solitons as they propagate inside the medium. Such two counter-propagating solitons meet somewhere inside the medium and interact. It is known that, in contrast to the pair of co-propagating solitons, this interaction is inelastic [15]. Mathematically, this means that two counter-propagating pulses do not form a stationary solution of the equations of motion. From the physical point of view, this fact can be explained with the simple argumentation as follows. For the co-propagating solitons, we always have a situation when the light energy absorbed at the leading edge of the pulse is released at its trailing edge. This is not the case for the counter-propagating solitons: at the point of collision, the medium excited at the leading edge of the first pulse interacts with the second pulse even before the trailing edge arrives. As a result, the collision of the pulses leads to the partial absorption of their energy.

It was recently shown [10] that, if $\Omega_{p1} = \Omega_0$ (2π -pulse) and $\Omega_{p2} = 1.5\Omega_0$ (3π -pulse), the FP soliton gets entirely absorbed, while the BP one appears unperturbed at the output. In other words, the first pulse is blocked by the second one. For simplicity, we call this situation the controlled absorption of light energy inside the two-level medium. This energy leaves the medium in a long run as a result of fluorescence. We should also emphasize that this effect occurs only for the asymmetric collision, i.e. when the amplitudes of both pulses are not the same.

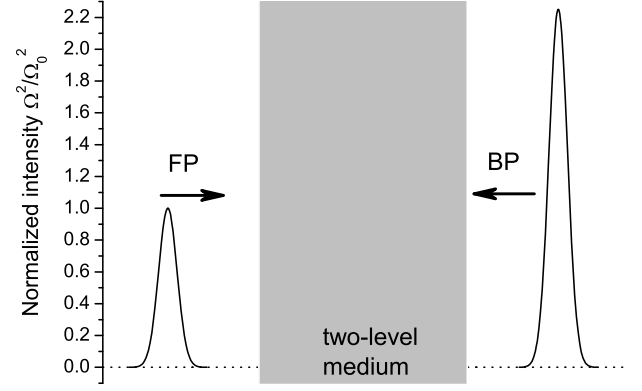


FIG. 1. The scheme of collision of two counter-propagating (FP and BP) pulses in a two-level medium.

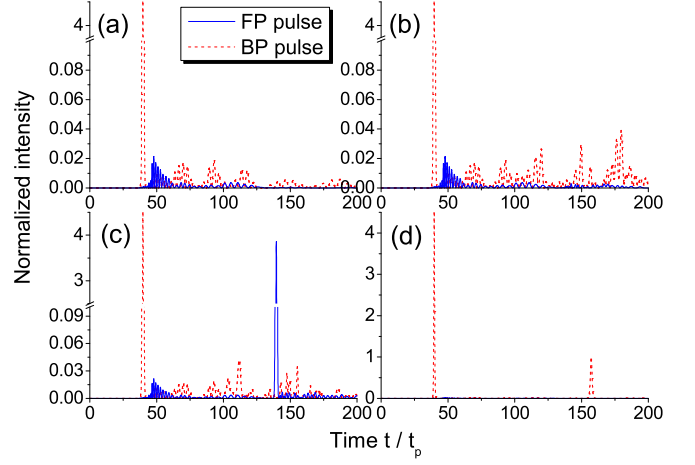


FIG. 2. (Color online) The resulting intensities after the collision: (a) collision of two pulses with $\Omega_{p1} = \Omega_0$ and $\Omega_{p2} = 1.5\Omega_0$; (b) the third (probe) FP pulse $\Omega_{p3} = \Omega_0$ is added; (c) the probe FP pulse has $\Omega_{p3} = 1.5\Omega_0$; (d) the probe pulse with $\Omega_{p3} = \Omega_0$ is BP. The first and second pulses start at the instant $t = 0$, while the third one starts at $t = 100t_p$.

The resulting profiles of the FP and BP pulses with initial amplitudes $\Omega_{p1} = \Omega_0$ and $\Omega_{p2} = 1.5\Omega_0$ are demonstrated in Fig. 2(a). These profiles are recorded at the opposite edges of the medium: according to Fig. 1, it is right edge for the FP pulse and the left edge for the BP one. One can easily see that the FP pulse is absent at the output (its energy is mostly absorbed), while the BP pulse appears at the other end of the medium. Note that this pulse (we can call it the control pulse) can be described by the usual 2π -soliton envelope and is significantly compressed in comparison with the initial pulse due to the transient process [10]. There are also low-intensity tails connected with radiation of absorbed light at both outputs of the medium.

III. DIODE ACTION

Now one can ask a question: what happens when the third (or probe) pulse with the amplitude Ω_{p3} enters the medium? There are three possible answers: (i) it will be trapped, (ii) it will pass through the medium, and (iii) it will not only pass but also retrieve the previously absorbed pulse from the medium. Further we try to investigate this question for different values of Ω_{p3} . If the possibility (iii) can be realized, one can talk about optical memory.

Let us add a probe pulse with amplitude Ω_{p3} which enters the medium after the interval $t = 100t_p$ when there is no propagating solitons inside the medium. There are two alternatives: the probe pulse is FP or BP. The case of FP probe pulse with $\Omega_{p3} = \Omega_0$ is shown in Fig. 2(b). It is seen that interaction of this pulse with the medium (which stores the energy of the previous FP pulse) prevents its appearance at the output. Only tails have somewhat increased intensity. As opposed to this case, the pulse $\Omega_{p3} = 1.5\Omega_0$ is happily transmitted through the medium though with slightly lower peak intensity than the identical BP pulse [Fig. 2(c)]. This means that transmittance of the soliton depends on its intensity. Moreover, we have an interesting deviation from the area theorem: the pulse with initial area 2π gets absorbed, while the one with 3π forms a 2π -soliton.

Now, if the probe pulse is BP and $\Omega_{p3} = \Omega_0$, then it appears at the output [Fig. 2(d)], in sharp contrast with the FP case [Fig. 2(b)]. In other words, the collision of two counter-propagating pulses switches the medium into such a state that it transmits the probe pulse incident from one side and blocks from the other. We can call this effect *the all-optical diode action*. The reason for this effect can be understood if we recall that the colliding pulses are not identical, i.e. the collision is asymmetric. As a consequence, this asymmetric collision "prepares" the asymmetric state of the medium, i.e. the diode action entirely depends on light-matter interaction, but not on the properly chosen geometry of the problem. Therefore, this scheme is fundamentally different from usual proposals of all-optical diodes based on asymmetrically constructed systems.

To study this asymmetry in more detail and to clarify the conditions for the diode action, we investigate the dependence of absorbed energy on the amplitude of the probe pulse Ω_{p3} (see Fig. 3). Absorbed energy is calculated as a part of total electromagnetic energy which remains inside the medium after some period (namely, $t = 200t_p$) from the start of the first two pulses. The curves for both (FP and BP) cases are situated between two asymptotes. The first one characterizes the fraction of the total energy of all three pulses which accounts for the first FP pulse. This asymptote is defined as the function $f_1(\Omega_{p3}) = \Omega_{p1}^2 / (\Omega_{p1}^2 + \Omega_{p2}^2 + \Omega_{p3}^2) = 1 / (3.25 + \tilde{\Omega}_{p3}^2)$, where we use the values $\Omega_{p1} = \Omega_0$, $\Omega_{p2} = 1.5\Omega_0$ and $\tilde{\Omega}_{p3} = \Omega_{p3}/\Omega_0$. It describes the absorbed energy in the ideal case when only the energy of the first pulse is

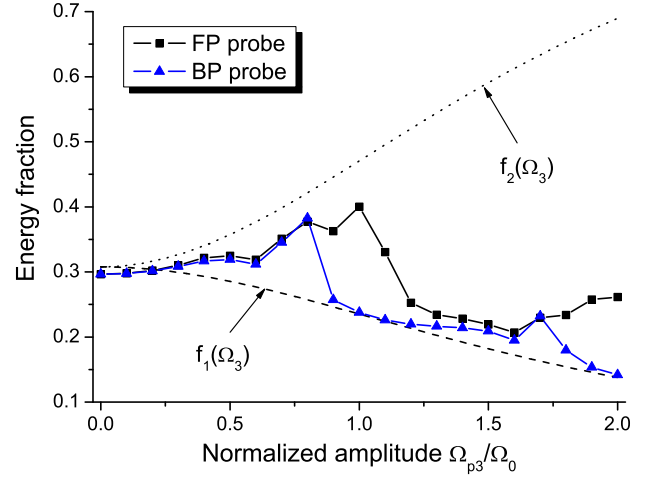


FIG. 3. (Color online) The dependence of absorbed energy (as a fraction of the total energy) on the amplitude Ω_{p3} of the probe pulse. The energy is integrated over the time period $t = 200t_p$.

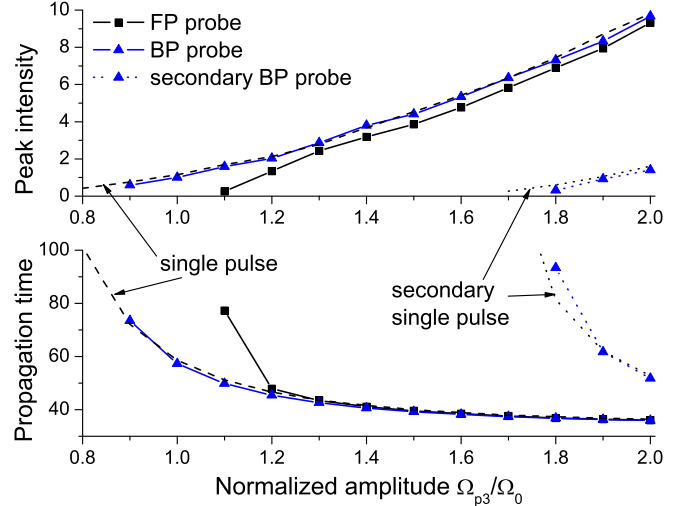


FIG. 4. (Color online) The dependence of peak intensity and propagation time (in units of t_p) on the amplitude Ω_{p3} of the probe pulse. For comparison, the results for a single pulse with the amplitude Ω_{p3} are shown.

trapped in the medium. Similarly, we introduce the second asymptote $f_2(\Omega_{p3}) = (\Omega_{p1}^2 + \Omega_{p3}^2) / (\Omega_{p1}^2 + \Omega_{p2}^2 + \Omega_{p3}^2) = (1 + \tilde{\Omega}_{p3}^2) / (3.25 + \tilde{\Omega}_{p3}^2)$, which describes the part of the energy carried by the first and third pulses together. It corresponds to another ideal situation when both the first and the probe pulses are absorbed.

It is seen in Fig. 3 that at low values of Ω_{p3} , the absorbed energy curves for the FP and BP probe pulses virtually coincide and are situated closer to the f_2 -asymptote, i.e. a large part of energy of the third pulse is absorbed inside the medium. However, at $\Omega_{p3} > 0.8\Omega_0$, the curves sharply diverge: the FP probe pulse is still mainly trapped, while the BP probe pulse is almost to-

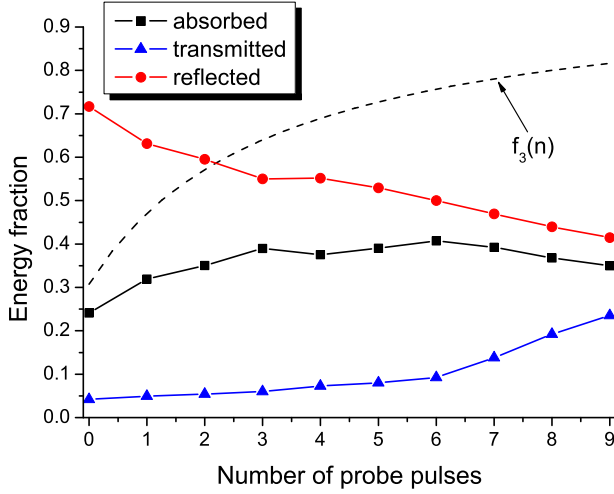


FIG. 5. (Color online) The dependence of absorbed, transmitted (FP), and reflected (BP) energy on the number of additional probe pulses with the amplitude Ω_0 . The energy is integrated over the time period $t = 1000t_p$.

tally transmitted (the blue curve with triangles gets very close to the f_1 -asymptote in Fig. 3). The energy of the first pulse is absorbed by the medium in both cases. Thus, the most distinction between the FP and BP cases is observed exactly in the region $\Omega_{p3} \approx \Omega_0$. This is the asymmetry seen in Figs. 2(b) and 2(d). At larger values of Ω_{p3} , the curves converge again, so that the medium becomes transparent for the FP pulse as well [cf. Fig. 2(c)]. Finally, for the FP pulses with $\Omega_{p3} \approx 2\Omega_0$, the fraction of trapped energy increases again. This allows us to see a certain periodicity of absorption, though we will not consider the case of large intensities ($\Omega_{p3} \geq 2\Omega_0$) here. One can expect more sophisticated dynamics in that case due to the process of pulse splitting into several 2π solitons.

The distinction between the FP and BP probe pulses is easily seen in Fig. 4, which shows the peak intensity of the probe pulse at the output versus its amplitude at the input. The BP probe pulse behavior almost coincides with that of the single pulse (i.e., with $\Omega_{p1} = \Omega_{p2} = 0$). On the contrary, the FP probe pulse has significantly lower value of peak intensity, which is equal to zero at $\Omega_{p3} < 1.5\Omega_0$ (no soliton at the exit). Note that at high input amplitudes, the secondary pulse appears as a result of pulse splitting of both the single and BP pulses. However, this is not the case for the FP probe pulse, i.e., the controlled absorption blocks the splitting of a high-intensity pulse in this case.

The next question to be discussed is as follows: How many FP pulses can be absorbed inside the medium? Obviously, the number must be limited. To find the answer, we launch a number of identical FP pulses (with $\Omega_{p3} = \Omega_0$) in $100t_p$ one after another and examine the fraction of absorbed energy as a function of probe pulse number n . The asymptote for ideal trapping of all the pulses is $f_3(n) = (\Omega_{p1}^2 + n\Omega_{p3}^2)/(\Omega_{p1}^2 + \Omega_{p2}^2 + n\Omega_{p3}^2) =$

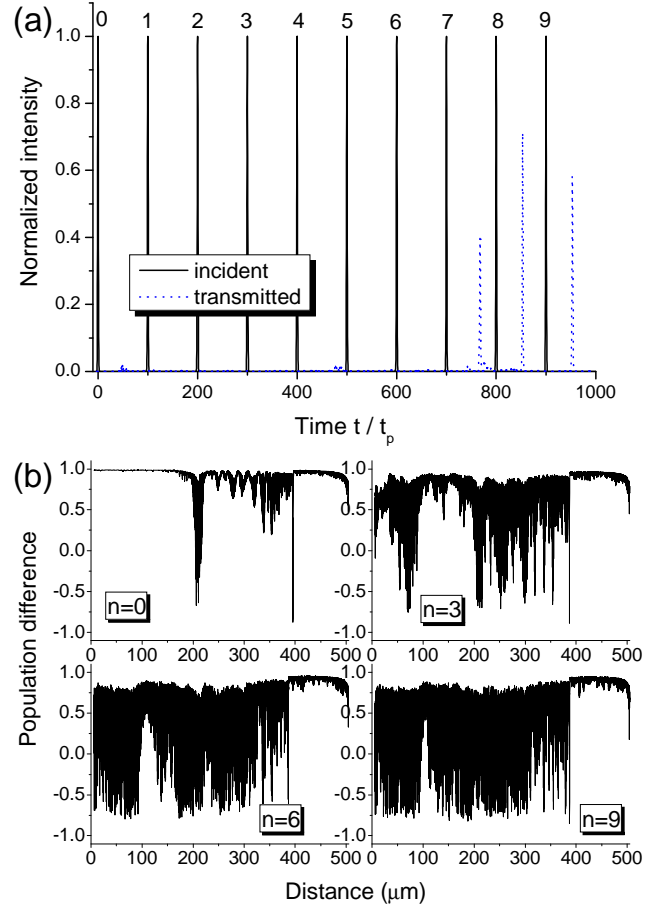


FIG. 6. (Color online) (a) Transmitted radiation profile for the nine incident probe pulses with the amplitude Ω_0 . (b) Distributions of population difference W inside the medium at the instant $t = 1000t_p$ for different numbers of probe pulses. Population difference $W = 1$ corresponds to atoms in the ground state.

$(1 + n)/(3.25 + n)$. The results of calculations for different n are presented in Fig. 5. It is seen that the difference between the asymptote and the absorption curve grows rapidly with n . Moreover, the absorbed energy stops increasing already at $n \geq 3$. This means that the saturation of light trapping takes place, while simultaneously the transmitted energy slowly grows. The increase of transmitted energy becomes significant at $n > 6$, while the absorbed part of the energy begins to decrease. One can expect that there should be not only the low-intensity tails at the output, but also the solitons as well. This expectation is proved to be valid by Fig. 6(a): there is no transmitted pulse at $n = 6$, but, starting from $n = 7$, every extra pulse appears at the output.

Figure 6(b) allows us to trace this saturation process. It is seen that the energy of the first absorbed pulse ($n = 0$) is localized inside the medium: medium excitation near $200 \mu\text{m}$ is due to the collision with the BP pulse, while the postcollisional pulse is trapped at larger distances (mainly, at $L < 400 \mu\text{m}$). As we launch addi-

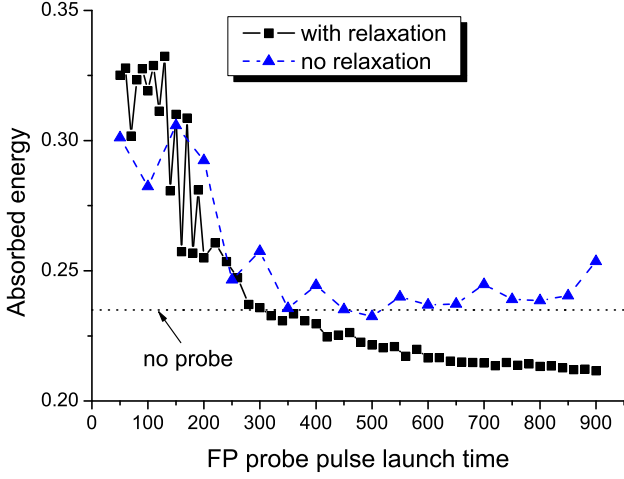


FIG. 7. (Color online) The dependence of absorbed energy (as a fraction of the total energy) on t_3 , the launch time of the probe FP pulse with amplitude $\Omega_{p3} = \Omega_0$. The energy is integrated over the time period $t = 1000t_p$. Time is measured in units of t_p .

tional (probe) FP pulses, their energy is absorbed in the unexcited regions of the medium ($n = 3$) until the distribution of excitation becomes practically uniform ($n = 6$). Note that the region $L > 400 \mu\text{m}$ remains almost unexcited, which was predetermined by the first pulse. This uniform distribution of population difference corresponds to the saturation and practically does not change when we add more pulses ($n = 9$). As a result, the interaction of the additional pulses gets weaker for $n > 7$, so that they can pass the medium. These smeared distributions also allow an understanding of why the absorbed pulse cannot be recovered. Therefore, we cannot talk about the storage of light and use the term "controlled absorption". The absorbed energy is radiated by the medium dipoles during the interval of the order of the relaxation time.

IV. PARAMETERS REGIONS FOR THE DIODE ACTION EXISTENCE

In the above consideration we adopted the time interval $100t_p$ between the launch instants of the first two and the third pulses. Here we must point out the significance of the time interval between the pulses, which must be much less than the relaxation times to preserve the coherence of light-matter interaction. We study this temporal effect in Fig. 7, which shows the absorbed part of the energy as a function of the launch time t_3 of the probe (second FP) pulse. The first two pulses were launched at the instant $t_1 = t_2 = 0$. It is seen that at short $t_3 < 200t_p$, absorbed energy is somewhere between the energy of the single FP Ω_0 pulse (0.235) and the energy of both FP Ω_0 pulses (0.47). This means that at the instant $t = 1000t_p$ (the final time of energy integration),

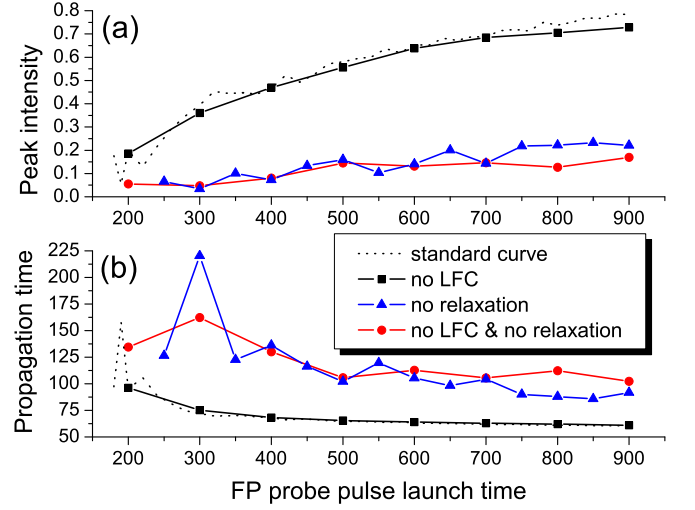


FIG. 8. (Color online) The dependence of (a) the peak intensity and (b) propagation time (in units of t_p) on t_3 , the launch time of the probe FP pulse with amplitude $\Omega_{p3} = \Omega_0$. The cases of absence of local-field correction (LFC) and relaxation are shown as well. The "standard curve" is calculated taking into account both LFC and relaxation.

the medium contains the energy of the first FP pulse and partly of the probe pulse. This absorbed energy slowly decreases as we increase the launch time t_3 , and at $t_3 > 300t_p$ it drops below the level of the single FP pulse energy. One can suggest the main role of relaxation in this behavior. Indeed, the time, say, $t = 500t_p = 25$ ps, is comparable with the relaxation time $T_2 = 100$ ps adopted in our calculations. To prove this suggestion, we performed simulations for the relaxation-free medium ($T_1 = T_2 = 0$). The results are presented in Fig. 7 (the dashed line with the triangles). It is seen that the curve in this case keeps above the level 0.235, i.e., the relaxation does not affect the process of controlled absorption of the first FP pulse. However, the energy of the probe pulse is not absorbed as well. Nevertheless, as Fig. 8 demonstrates, the peak intensity of the pulse transmitted is strongly suppressed for the relaxation-free medium in comparison with the case of the presence of relaxation (this last case is shown by the "standard curve" in the figure). Thus, relaxation helps to form an intense soliton during propagation through the medium prepared by the collision of two counter-propagating pulses.

Figure 8 also clarifies the influence of local-field correction [the nonlinear addition to the detuning in Eq. (1)] on the effects discussed. It is seen that this influence can be considered as negligible for our parameters. This is in full accordance with the conclusion of Ref. [13]. Indeed, for the parameters of our calculations ($\omega_L = 10^{11} \text{ s}^{-1}$, $t_p = 50$ fs), the ratio of the pulse amplitude (peak Rabi frequency) to the Lorentz frequency is $\Omega_0/\omega_L = \sqrt{2\pi} \cdot 10^2 \gg 1$, while, for the local-field effects to be observed, one needs $\Omega_0/\omega_L \sim 1$.

Now let us consider the effect of pulse duration on the

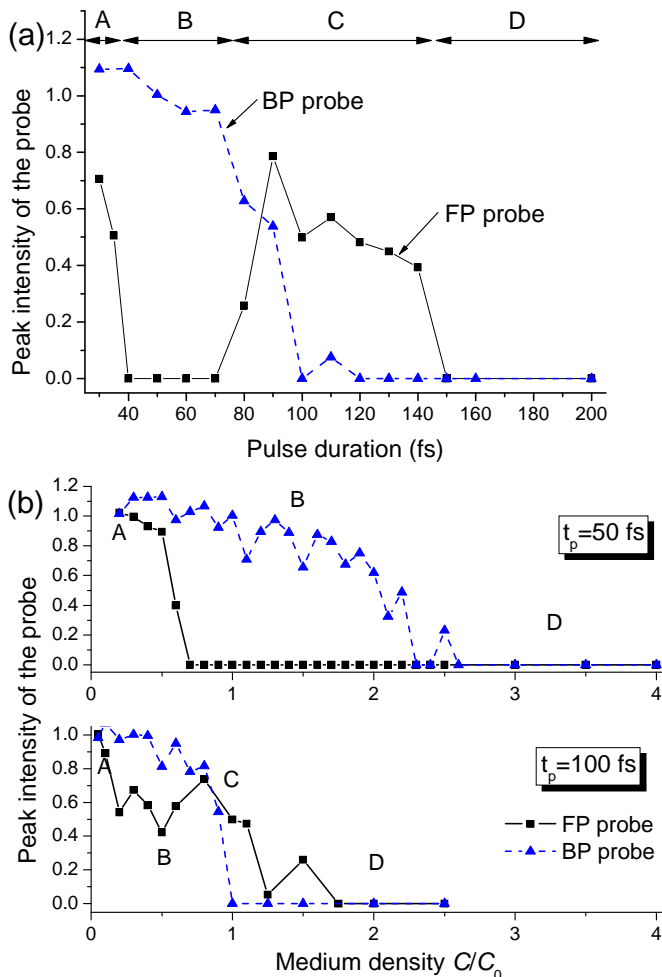


FIG. 9. (Color online) The dependence of the peak intensity of the probe pulse on (a) the duration of the pulses, and (b) the density of the medium (for two different durations). The value C_0 used for normalization corresponds to the Lorentz frequency $\omega_L = 10^{11} \text{ s}^{-1}$. In figure (a) the value $C = C_0$ is adopted.

controlled absorption and all-optical diode action. The results of calculations are depicted in Fig. 9(a). We mark out there several regions denoted with letters from A to D. In region A (very short pulses, $t_p < 30$ fs) both FP and BP probe pulses appear at the output. Moreover, the total absorption of the first FP soliton is not observed in this case. Therefore, one can say that region A is the region of elastic collisions of the counter-propagating solitons, which is characteristic for short enough (high-intensity) pulses [10, 16]. The region D (long pulses, $t_p > 150$ fs) is the reverse case of strongly inelastic collisions, so that the soliton is annihilated independently of the propagation direction [16]. Finally, the intermediate regions B and C are of interest for us. In region B (conditions considered above in this paper), the FP probe pulse is absorbed, while the BP one is transmitted. In region C the situation is reversed, so that one can change the direction of the diode action simply by changing the

duration of the incident pulses.

Obviously, the dynamics of light depend not only on the parameters of the pulses themselves, but also on the parameters of the medium, such as its density. In other words, the behavior of the soliton inside the medium is governed by the combination of the field and matter characteristics. In the paper [15], the combination $\Upsilon \sim Ct_p^2$ was proposed, so that for longer pulses, one can obtain the effect at lower density. We study this relationship in Fig. 9(b), where the probe pulse peak intensity is plotted versus the medium density (in units of C_0 corresponding to the previously used Lorentz frequency $\omega_L = 10^{11} \text{ s}^{-1}$). One can see that at $t_p = 50$ fs, the diode action covers a wide region of densities $0.7 < C/C_0 < 2.3$ [B region, in terms of Fig. 9(a)]. At lower and higher densities, there is no directional asymmetry in pulse behavior (elastic and strongly inelastic conditions, respectively). If we take longer pulses ($t_p = 100$ fs), region B shifts toward lower densities and becomes narrower, in accordance with the Υ combination. It is also important that the contrast between the curves in region B is not as impressive as for shorter pulses. However, we can say with confidence that the asymmetric propagation appears at lower densities than previously due to the increase in pulse duration. In addition, a narrow C region appears at $t_p = 100$ fs, while region A is located near the very vertical axis. In general, the Υ combination satisfactorily describes the effects of density and pulse duration on the location and width of the region of the diode action.

V. CONCLUSION

In conclusion, we studied the collisions of multiple counter-propagating SIT solitons within the framework of the semiclassical model of light interaction with a homogeneously broadened two-level medium. It is shown that by means of inelastic asymmetric collision of two proper pulses, the medium can be prepared in such a state that it behaves as a diode transmitting the probe pulse or not, depending on propagation direction and peak intensity. This medium preparation is connected with the controlled light absorption in the medium which is limited by the process of saturation. By combining the characteristics of the medium and the pulse, one can find the proper conditions to observe the effects of asymmetric collisions. We should also notice that pulse retrieval was not achieved, so that the stored energy leaves the medium naturally as a consequence of fluorescence.

One can expect that the effects of SIT solitons collisions can be observed in usual self-transparency media: solid dielectrics (including ruby where SIT was first discovered), vapors of alkali metals, molecular gases, and semiconductors. A review of the early experiments can be found in Ref. [9]. Obviously, the solid-state systems seem to be the most convenient for our aims. The conditions considered in this paper (very short and high-intensity pulses, short distances of propagation) are in

good agreement with the requirements of semiconductor materials which possess short relaxation times and comparatively high transition dipole moments. The theoretical and experimental results on self-induced transmission in semiconductors were reported, for example, in [17–20]. Another prospective material for SIT collision experiments is the collection of semiconductor quantum dots which can be considered as artificial two-level atoms with high dipole moments [21, 22].

The final remark deals with the problem of inhomogeneous broadening when the resonant frequency of two-level atoms is distributed in a certain range. Recall that our calculations were performed for the case of a homoge-

neously broadened medium, i.e., for broadening only due to the finite phenomenological relaxation T_2 (equal for every atom). As a matter of fact, we are in the well-studied regime of SIT solitons which have essentially the same main properties in both cases of homogeneous and inhomogeneous broadening [9]. Moreover, the well-known area theorem (one of the attributes of SIT) is not valid in a strict sense for the homogeneously broadened medium [9], as it was confirmed recently by direct numerical simulations [23]. Therefore, although the role of inhomogeneous broadening is still to be studied, we believe that the main features of SIT pulse collisions should remain unchanged in that case.

-
- [1] K. Gallo and G. Assanto, *J. Opt. Soc. Am.* **B16**, 267 (1999).
 - [2] S. V. Zhukovsky and A. G. Smirnov, *Phys. Rev.* **A83**, 023818 (2011).
 - [3] C. Lu, X. Hu, Y. Zhang, Z. Li, X. Xu, H. Yang, and Q. Gong, *Appl. Phys. Lett.* **99**, 051107 (2011).
 - [4] C. Xue, H. Jiang, and H. Chen, *Opt. Express* **18**, 7479 (2010).
 - [5] X. Cai, X. Wang, and S. Li, *Opt. Commun.* **285**, 1959 (2012).
 - [6] M. W. Feise, I. V. Shadrivov, and Y. S. Kivshar, *Phys. Rev.* **E71** 037602 (2005).
 - [7] R. Philip, M. Anija, C. S. Yelleswarapu, and D. V. G. L. N. Rao, *Appl. Phys. Lett.* **91** 141118 (2007).
 - [8] S. L. McCall and E. L. Hahn, *Phys. Rev.* **183**, 457 (1969).
 - [9] I. A. Poluektov, Yu. M. Popov, and V. S. Roitberg, *Sov. Phys. Usp.* **17**, 673 (1975).
 - [10] D. V. Novitsky, *Phys. Rev.* **A84**, 013817 (2011).
 - [11] C. M. Bowden and J.P. Dowling, *Phys. Rev.* **A47**, 1247 (1993).
 - [12] M. E. Crenshaw, *Phys. Rev.* **A54**, 3559 (1996).
 - [13] D. V. Novitsky, *Phys. Rev.* **A82**, 015802 (2010).
 - [14] D. V. Novitsky, *Phys. Rev.* **A79**, 023828 (2009).
 - [15] M. J. Shaw and B. W. Shore, *J. Opt. Soc. Am.* **B8**, 1127 (1990).
 - [16] A. A. Afanas'ev, V. M. Volkov, V. M. Dritz, and B. A. Samson, *J. Mod. Opt.* **37**, 165 (1990).
 - [17] H. Giessen, A. Knorr, S. Haas, S. W. Koch, S. Linden, J. Kuhl, M. Hetterich, M. Grün, and C. Klingshirn, *Phys. Rev. Lett.* **81**, 4260 (1998).
 - [18] N. C. Nielsen, S. Linden, J. Kuhl, J. Förstner, A. Knorr, S. W. Koch, and H. Giessen, *Phys. Rev.* **B64**, 245202 (2001).
 - [19] N. C. Nielsen, T. Höner zu Siederdissen, J. Kuhl, M. Schaarschmidt, J. Förstner, A. Knorr, and H. Giessen, *Phys. Rev. Lett.* **94**, 057406 (2005).
 - [20] O. A. Smyrnov and F. Biancalana, *Phys. Rev.* **B85**, 075201 (2012).
 - [21] G. Panzarini, U. Hohenester, and E. Molinari, *Phys. Rev.* **B65**, 165322 (2002).
 - [22] S. Schneider, P. Borri, W. Langbein, U. Woggon, J. Förstner, A. Knorr, R. L. Sellin, D. Ouyang, and D. Bimberg, *Appl. Phys. Lett.* **83**, 3668 (2003).
 - [23] X. Y. Yu, W. Liu, and C. Li, *Phys. Rev.* **A84**, 033811 (2011).